10.64837/GSA.13.5.3

Global and Stochastic Analysis
Vol. 13 No. 5 (2026)
Received: 20th June 2026 Revised: 19th August 2026 Accepted: 08th September 2026

FRACTIONAL MEAN-FIELD INTERVAL TYPE-2 FUZZY STOCHASTIC CONTROL FOR CARBON-AWARE EDGE-CLOUD NETWORKS UNDER RENEWABLE-ENERGY UNCERTAINTY

YOGEESH NIJALINGAPPA*, TAHIR MUHAMMAD ALI, ASOKAN VASUDEVAN, HEKPAZO ROMARIC C. MARC, AND JONATHAN LEE

Abstract. A fractional mean-field stochastic control model is developed for carbon-aware edge-cloud networks operating under renewable generation, grid-carbon, electricity-price and workload uncertainty. The proposed controller combines Caputo memory, interval type-2 fuzzy uncertainty envelopes, graph-coupled mean-field interaction, Wasserstein distributional robustness and conditional value-at-risk. The state process includes reflected queues, battery storage, processor frequency and carbon exposure. The optimality equations are written as a coupled Hamilton-Jacobi-Bellman-Fokker-Planck system with a projection step that preserves routing, service, battery and thermal feasibility. Existence, mean-square boundedness and convergence of a projected fixed-point iteration are established under explicit Lipschitz, compactness and Slater-type conditions. A self-contained 20-scenario benchmark is reported in the manuscript. The proposed fractional mean-field interval type-2 stochastic controller reduces mean SOC-neutral carbon by 14.99% relative to round-robin, 12.97% relative to carbon-greedy routing and 11.42% relative to renewable-aware MPC, while keeping mean delay below 0.06 minutes.

1. Introduction

Energy-efficient computing is no longer sufficient for sustainable digital infrastructure. A kilowatt-hour consumed at different hours or locations can produce very different operational emissions. Edge-cloud networks add a further layer of difficulty because routing decisions, local renewable availability, queueing delay, battery state, processor frequency and thermal effects interact over time. The carbon-minimising action at the current instant can be poor over a full horizon when it drains storage, creates backlog or exposes the system to later high-carbon grid periods. The problem is therefore a constrained stochastic control problem on a graph rather than a static ranking problem.

Three mathematical issues motivate the present study. First, renewable and carbon forecasts contain both stochastic variation and epistemic uncertainty. The former can be represented by random scenarios, whereas the latter requires uncertainty about the membership grade or confidence in the forecast itself. Interval

2010 *Mathematics Subject Classification.* Primary 60H10, 60G22, 90C15; Secondary 03E72, 68M20, 91A16, 93E20.

Key words and phrases. fractional stochastic control, interval type-2 fuzzy sets, mean-field games, carbon-aware computing, Wasserstein ambiguity, CVaR, edge-cloud networks.

*Corresponding author.

Corresponding author: YOGEESH NIJALINGAPPA (Email address: yogeesh.r@gmail.com)

type-2 fuzzy sets give a natural representation of this second layer through a footprint of uncertainty [12, 14, 18, 19, 30]. Second, workload and resource decisions are coupled by an edge-cloud topology. A node-level controller that ignores graph structure cannot fully represent migration, congestion and shared infrastructure effects. Graph neural and mean-field models provide scalable alternatives for large networks [3, 8, 13, 23]. Third, carbon-aware decisions should account for adverse tails. Expected emissions alone may select policies that are favourable on average but exposed to rare high-carbon periods. Wasserstein distributional robustness and CVaR risk offer convex instruments for this purpose [9, 21, 22, 24, 28].

The paper develops a fractional mean-field interval type-2 stochastic controller for carbon-aware edge-cloud operation. Fractional memory is included because workload, battery and thermal states exhibit path dependence. Rather than treating this memory only as a computational device, the fractional order appears directly in the state dynamics and the optimality system. The benchmark is self-contained: every numerical parameter and scenario-level output used for the reported claims appears in the tables of the paper. This avoids hidden dependence on external files and makes the computational record available to the reader inside the manuscript.

The main contributions are as follows. First, a Caputo-memory reflected stochastic model is formulated for queues, storage and carbon-aware edge-cloud control. Second, an interval type-2 fuzzy layer is embedded in a Wasserstein-CVaR risk functional. Third, the limiting population interaction is expressed through a fractional HJB-FPK fixed point. Fourth, well-posedness, Lyapunov boundedness and projected fixed-point convergence are proved. Fifth, a complete numerical record is included, with benchmark parameters, scenario outputs, sensitivity values and ablation results.

2. Related mathematical and computational foundations

Edge computing has been motivated by the need to process data near users while reducing latency and communication pressure [16, 17, 25]. Energy-aware cloud control developed consolidation, frequency scaling and resource allocation principles [2, 5]. Carbon-aware data-centre operation then shifted attention from energy minimisation alone to temporal and geographic variation in carbon intensity [1, 7, 10, 11, 15, 26, 29]. These studies show why workload placement must be linked to grid and renewable conditions. They do not, by themselves, resolve the mathematical difficulty created by path dependence, epistemic forecast uncertainty and tail-risk control.

Fractional calculus provides a compact representation of memory effects. The Caputo derivative is useful in control models because it permits classical initial conditions [4, 6, 20]. In the present setting, memory is not interpreted as a physical law for every server component. It is used as a parsimonious kernel for persistent workload, thermal and storage effects that influence control decisions across a day. The numerical sensitivity study in Section 8 shows that the fractional order materially changes carbon and residual behaviour.

Interval type-2 fuzzy logic generalises type-1 membership by allowing the grade itself to vary inside an interval. The corresponding footprint of uncertainty separates nominal membership from membership uncertainty [12, 14, 18, 19]. This distinction

is important for carbon-aware computing: a forecast may be numerically precise but not reliable, or it may be imprecise but consistently conservative. The proposed model passes both the type-reduced centre and the interval width into the risk functional.

Mean-field models describe the effect of a large population through a distributional state. Their HJB-FPK structure is well suited to networks where each node responds to aggregate congestion and energy conditions [13]. Wasserstein distributional robustness protects against probability-law misspecification [9, 21, 24, 28], while CVaR focuses on high-loss tails [22]. The contribution lies in the coupled fractional, fuzzy, mean-field and robust stochastic-control system, supported by a complete set of numerical results.

3. Fractional stochastic edge-cloud model

Let $G = (V, E, A)$ be a directed weighted edge-cloud graph with $n = |V|$ nodes. The entries a_{ij} encode feasible task migration and information exchange. Let $D = \operatorname{diag}(A\mathbf{1})$ and $L = D - A$ denote the graph Laplacian. For a sufficiently smooth scalar process x, the Caputo derivative of order $0 < \beta \leq 1$ is

$$D_t^{\beta,C} x(t) = \frac{1}{\Gamma(1-\beta)} \int_0^t (t-s)^{-\beta} \frac{dx(s)}{ds}\, ds\,. \tag{3.1}$$

At node i, the state vector is

$$X_i(t) = (q_i(t), s_i(t), \theta_i(t), r_i(t), c_i(t), p_i(t))\,, \tag{3.2}$$

where q_i is backlog, s_i battery energy, θ_i thermal state, r_i renewable availability, c_i grid-carbon intensity and p_i electricity price. The control vector is

$$U_i(t) = \big(u_i(t), b_i^{ch}(t), b_i^{dis}(t), \rho_{ij}(t), f_i(t), z_i(t)\big)\,, \tag{3.3}$$

where u_i is served work, b_i^{ch} and b_i^{dis} are charge and discharge rates, ρ_{ij} is routed work, f_i is normalised processor frequency and $z_i \in [0,1]$ is a relaxed active-state variable.

The fractional reflected queue dynamics are

$$D_t^{\beta,C} q_i(t) = \lambda_i(t) + \sum_j a_{ji}\rho_{ji}(t) - u_i(t) - \sum_j a_{ij}\rho_{ij}(t) + \zeta_i^q(t), \quad q_i(t) \geq 0\,. \tag{3.4}$$

The battery evolves according to

$$D_t^{\beta,C} s_i(t) = \eta_c b_i^{ch}(t) - \frac{b_i^{dis}(t)}{\eta_d} - \kappa_i s_i(t) + \zeta_i^s(t), \quad 0 \leq s_i(t) \leq B_i\,. \tag{3.5}$$

The terms ζ_i^q and ζ_i^s collect Brownian perturbations and reflection increments for the queue and battery boundaries.

The nonlinear information-technology power is

$$P_i^{IT}(t) = z_i(t) P_i^{idle} + \alpha_i f_i(t)^3 \left(\frac{u_i(t)}{\bar{u}_i}\right)^{\gamma_i} + \chi_i \left|u_i(t) - u_i(t-\Delta t)\right|\,. \tag{3.6}$$

Grid power is evaluated after renewable use and storage dispatch:

$$P_i^{grid}(t) = \max\{P_i^{IT}(t) + P_i^{cool}(t) - r_i(t) - b_i^{dis}(t) + b_i^{ch}(t), 0\}\,. \tag{3.7}$$

The instantaneous operational carbon rate is

$$C(t) = \sum_{i=1}^{n} c_i(t) P_i^{grid}(t)\,. \tag{3.8}$$

Equations (3.1)–(3.7) define the fractional stochastic state model. The reflection terms K_i^q, K_i^0, K_i^B are minimal nondecreasing processes enforcing the queue and battery boundaries.

4. Interval type-2 fuzzy uncertainty layer

Let $\widetilde{A}$ be an interval type-2 fuzzy set on a domain $\mathcal{X}$. It is represented as

$$\widetilde{A} = \{\Big(x, \Big[\underline{\mu}_A(x), \overline{\mu}_A(x)\Big]\Big) : x \in \mathcal{X}\} \tag{4.1}$$

For a forecast feature x_{ik}, the upper and lower memberships are chosen as

$$\overline{\mu}_{ik}(x) = \exp\left[-\frac{(x - m_{ik})^2}{2\,(\sigma_{ik} + \delta_{ik})^2}\right], \qquad \underline{\mu}_{ik}(x) = h_{ik} \exp\left[-\frac{(x - m_{ik})^2}{2\,(\sigma_{ik} - \delta_{ik})^2}\right]. \tag{4.2}$$

The footprint width is updated from rolling forecast error and model disagreement:

$$\delta_{ik}(t) = \delta_{ik}^{\min} + \omega_1\, \mathrm{MAD}_w\,(e_{ik}) + \omega_2 \left|\widehat{x}_{ik}^{(1)} - \widehat{x}_{ik}^{(2)}\right|. \tag{4.3}$$

For rule r, the interval firing strength is

$$F_r(x) = \Big[\underline{f}_r(x), \overline{f}_r(x)\Big] = \left[\prod_{k=1}^{p} \underline{\mu}_{rk}\,(x_k)\,, \prod_{k=1}^{p} \overline{\mu}_{rk}\,(x_k)\right]. \tag{4.4}$$

With affine consequent $y_r(x) = \theta_r^{\top}\left(1, x^{\top}\right)^{\top}$, center-of-sets type reduction gives

$$y_L = \min_{f_r \in [\underline{f}_r, \overline{f}_r]} \frac{\sum_r f_r y_r}{\sum_r f_r}, \qquad y_R = \max_{f_r \in [\underline{f}_r, \overline{f}_r]} \frac{\sum_r f_r y_r}{\sum_r f_r}\,. \tag{4.5}$$

The controller uses $y_c = (y_L + y_R)/2$ as the nominal uncertainty feature and $y_w = (y_R - y_L)/2$ as an epistemic risk feature. Thus, the type-2 layer does not eliminate uncertainty during defuzzification; it exposes the width of uncertainty to the robust objective.

The diagram shows how stochastic inputs are transformed by the type-2 fuzzy layer and fractional memory state before entering the mean-field robust controller.

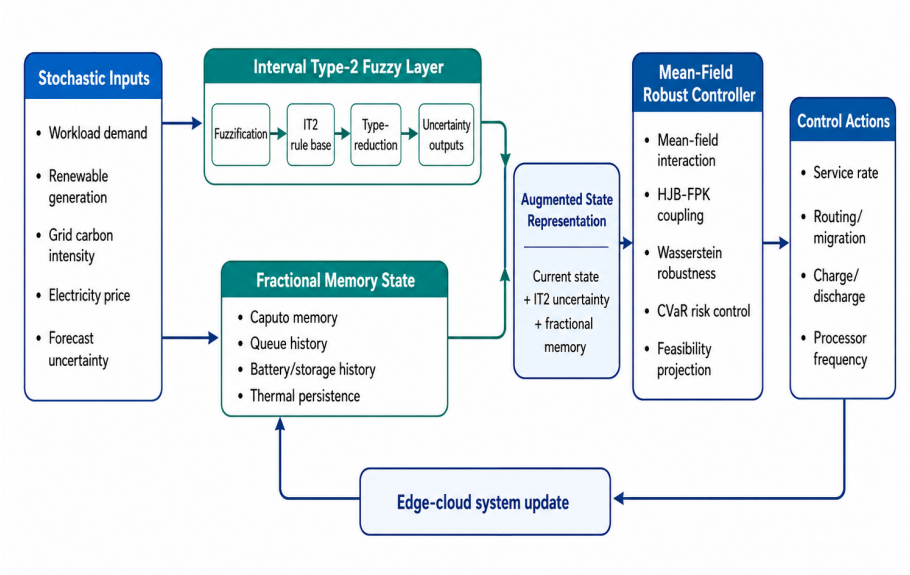


FIGURE 1. Fractional mean-field interval type-2 stochastic control architecture.

5. Mean-field robust control formulation

Let m_t denote the empirical distribution of node states at time t. For a test function φ, the population law is

$$\langle m_t, \varphi \rangle = \frac{1}{n} \sum_{i=1}^{n} \varphi\left(X_i(t)\right) . \tag{5.1}$$

The control policy is parameterised as

$$U_i(t) = \Pi_{\mathcal{U}_i(X_i, m_t)} \left[g_\vartheta \{ X_i(t), m_t, y_{c,i}(t), y_{w,i}(t) \} \right] . \tag{5.2}$$

The projection is taken in the metric of the feasible set containing routing, service, frequency, battery, thermal and delay constraints. The baseline loss over $[0, T_f]$ is

$$Z(U, \xi) = \int_0^{T_f} C(t; U, \xi)\, dt + \omega_q \int_0^{T_f} \| \, q(t) \, \|_1 \, dt + \omega_p \int_0^{T_f} p(t)^\top P^{grid}(t)\, dt \, . \tag{5.3}$$

Let $\widehat{\mathbb{P}}_N = N^{-1} \sum_{s=1}^{N} \delta_{\widehat{\xi}_s}$ be the empirical distribution of benchmark scenarios. The Wasserstein ambiguity set is

$$\mathcal{B}_\varepsilon \left(\widehat{\mathbb{P}}_N \right) = \left\{ \mathbb{Q} : W_1 \left(\mathbb{Q}, \widehat{\mathbb{P}}_N \right) \leq \varepsilon \right\} . \tag{5.4}$$

The CVaR of a loss Z is written in the convex form

$$\mathrm{CVaR}_\alpha(Z) = \min_{\eta \in \mathbb{R}} \left[\eta + \frac{1}{1-\alpha} \mathbb{E}\, \psi_\eta(Z) \right] , \quad \psi_\eta(Z) = \max\{Z - \eta, 0\} . \tag{5.5}$$

The robust fractional mean-field control problem is

$$J_{opt} = \min_{\vartheta,U,\eta} \max_{\mathbb{Q}\in\mathcal{B}_\varepsilon} \left[\mathbb{E}_{\mathbb{Q}} Z(U,\xi) + \omega_r \,\mathrm{CVaR}_\alpha^{\mathbb{Q}}(Z) + \omega_s R_s(U) + \omega_g R_g(U)\right] . \tag{5.6}$$

The HJB equation for the representative node has the form

$$\begin{aligned} -D_t^{\beta,C} V(x,t) &= \min_{u\in\mathcal{U}(x,m_t)} \left[\ell(x,u,m_t) + \mathcal{L}^u V(x,t) + \Phi(x,u,m_t)\right], \\ V(x,T_f) &= G(x,m_{T_f}). \end{aligned} \tag{5.7}$$

The corresponding Fokker-Planck equation is

$$D_t^{\beta,C} m_t = -\nabla\cdot\left(b\left(x,u_t(x),m_t\right) m_t\right) + \frac{1}{2}\nabla^2 : \left(\Sigma\Sigma^\top\left(x,u_t(x),m_t\right) m_t\right) . \tag{5.8}$$

The pair (5.7)–(5.8) defines a fractional HJB-FPK fixed point. The control is then projected onto the physically feasible set to obtain implementable node actions.

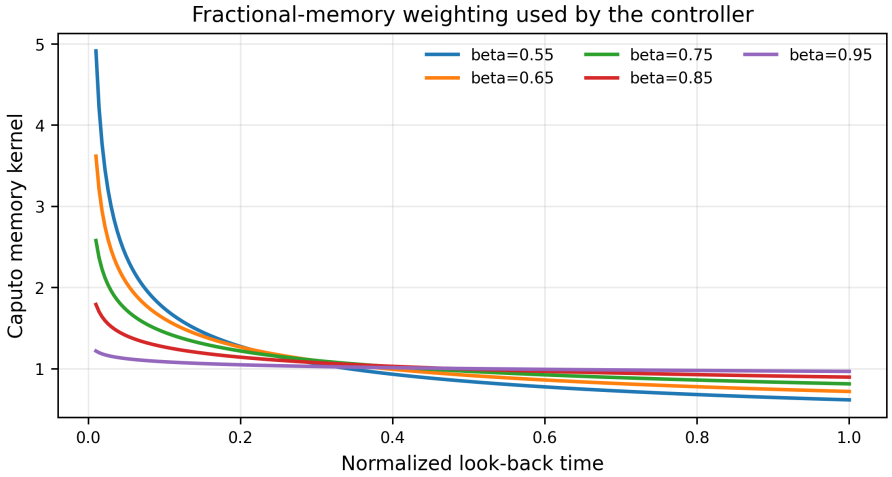


FIGURE 2. Fractional-memory kernels for different orders.

Smaller values of β place stronger weight on older states, while β close to one approaches a short-memory differential model.

6. Analytical properties

The analysis uses the following standing assumptions. The arrival, renewable, carbon and price processes have finite second moments. Drift and diffusion functions are globally Lipschitz with linear growth. The feasible set is nonempty, compact and convex after the standard relaxation of charge-discharge complementarity. The graph Laplacian is positive semidefinite. The type-reduced fuzzy features are bounded and Lipschitz in the forecast vector. A Slater policy exists for the average delay and battery constraints.

Theorem 6.1 (Well-posed fractional reflected state)**.** *Under the stated assumptions, the system* (3.3)–(3.7) *has a unique strong reflected solution on* $[0, T_f]$ *for every progressively measurable feasible control. Moreover,* $q_i(t) \geq 0$ *and* $0 \leq s_i(t) \leq B_i$ *almost surely.*

Proof. The Caputo state can be written in Volterra integral form with kernel $(t-s)^{\beta-1}/\Gamma(\beta)$. Lipschitz drift and diffusion give contraction on a sufficiently short interval. Iteration over finitely many subintervals yields existence and pathwise uniqueness. The queue orthant and battery box are convex domains with Lipschitz Skorokhod maps, so composition of the unconstrained Volterra solution with the reflection map preserves uniqueness and enforces the boundary conditions. □

Define the Lyapunov function

$$\mathcal{V}(q, s) = \frac{1}{2} \parallel q \parallel_2^2 + \frac{\nu}{2} \parallel s - s_0 \parallel_2^2 . \tag{6.1}$$

If there exists $\epsilon > 0$ such that the robust service margin satisfies

$$\mathbb{E}\left[u + B\rho - \lambda \mid X, m_t\right] \succcurlyeq \epsilon \mathbf{1} \quad \text{whenever} \quad \parallel q \parallel_1 > Q_0, \tag{6.2}$$

then the fractional generator satisfies

$$D_t^{\beta, C} \mathbb{E}\left[\mathcal{V}\left(q(t), s(t)\right)\right] \leq B_0 - \epsilon_0 \mathbb{E} \parallel q(t) \parallel_1 . \tag{6.3}$$

Theorem 6.2 (Mean-square boundedness)**.** *If* (6.2) *holds, then*

$$\limsup_{T \to \infty} \frac{1}{T} \int_0^T \mathbb{E} \parallel q(t) \parallel_1 dt \leq \frac{B_0}{\epsilon_0} . \tag{6.4}$$

Proof. Apply the fractional Itô–Volterra formula to (6.1). The reflected terms do not add positive interior drift because the queue reflection acts only when $q_i = 0$. Diffusion traces and bounded storage terms are absorbed into B_0. The service margin gives the negative linear drift outside a compact set. Fractional Gronwall bounds and Cesaro averaging prove (6.4).

The projected fixed-point iteration is

$$\begin{aligned} U_{k+1} &= \Pi_{\mathcal{U}}\big(U_k - \tau_k \left[\nabla F(U_k) + Jg(U_k)^\top \lambda_k\right]\big) , \\ \lambda_{k+1} &= \max\{0, \lambda_k + \sigma_k g(U_{k+1})\}. \end{aligned} \tag{6.5}$$

Theorem 6.3 (Projected fixed-point convergence)**.** *Suppose the sample-average robust objective is convex with* L_F*-Lipschitz gradient,* g *is affine and a saddle point exists. If* $0 < \tau < 2/L_F$ *and* $0 < \tau\sigma \parallel Jg \parallel^2 < 1$*, then the averaged iterates satisfy*

$$F\left(\overline{U}_K\right) - F\left(U_{opt}\right) + \parallel \max\left(0, g\left(\overline{U}_K\right)\right) \parallel_1 = O\left(K^{-1}\right) . \tag{6.6}$$

Proof. Firm nonexpansiveness of projection and cocoercivity of ∇F give a one-step contraction of the primal-dual gap up to a summable residual. Telescoping the resulting inequality and applying Jensen's inequality to the averaged iterate yields (6.6).

7. Benchmark design and numerical record

The benchmark uses 12 heterogeneous nodes, 96 fifteen-minute intervals and 20 independent day scenarios. The compared controllers are round-robin grid scheduling, carbon-greedy routing, renewable-aware MPC, type-1 fuzzy scheduling and the proposed fractional mean-field interval type-2 stochastic controller. Terminal state-of-charge normalisation is used so that a controller cannot reduce apparent emissions by emptying the battery at the end of the horizon. The SOC-neutral correction is

$$Z^{neutral} = Z^{direct} + \left(E_S^0 - E_S^T\right) \overline{C}_{end} \,. \tag{7.1}$$

For a scenario-level metric z_s, the reported mean and sample standard deviation are

$$\overline{z} = \frac{1}{N_{MC}} \sum_{s=1}^{N_{MC}} z_s, \qquad s_z = \left(\frac{1}{N_{MC}-1} \sum_{s=1}^{N_{MC}} (z_s - \overline{z})^2 \right)^{1/2} . \tag{7.2}$$

Table 1 gives the node classes. Table 2 gives the main aggregate results. Tables 3–7 give the complete scenario outputs used to obtain the reported carbon, energy, cost, delay and renewable-utilization values. Tables 8–10 give reduction, fractional-order sensitivity and ablation records.

Table 1. Node classes used in the benchmark.

Node class	Count	Service cap range	Idle power kW	Dynamic coeff	Battery kWh
Micro edge	4	[120,180]	1.10	2.40	35
Campus edge	4	[180,260]	1.80	3.10	60
Regional edge	3	[260,360]	2.70	4.00	110
Cloud gateway	1	[520,620]	5.40	8.60	180

Table 2. Aggregate performance over 20 scenarios.

Controller	Carbon mean	Carbon SD	Grid energy mean	Cost mean	Delay mean	Renewable mean
RR-Grid	3150.261	187.266	6397.434	556.198	0.037	37.277
Carbon-Greedy	3077.226	179.620	6425.419	566.447	2.081	37.279
Renewable-MPC	3023.502	182.592	5972.504	520.217	0.099	39.129
Type-1 Fuzzy	3561.412	222.696	7309.967	635.364	0.403	34.733
FMF-IT2-SC	2678.073	167.056	5258.555	455.151	0.056	43.587

Error bars denote one sample standard deviation computed from the scenario values in Table 3.

The proposed controller remains below the compared baselines across the evaluated stochastic scenarios.

The proposed controller is located in the low-carbon and low-delay region of the evaluated controller set.

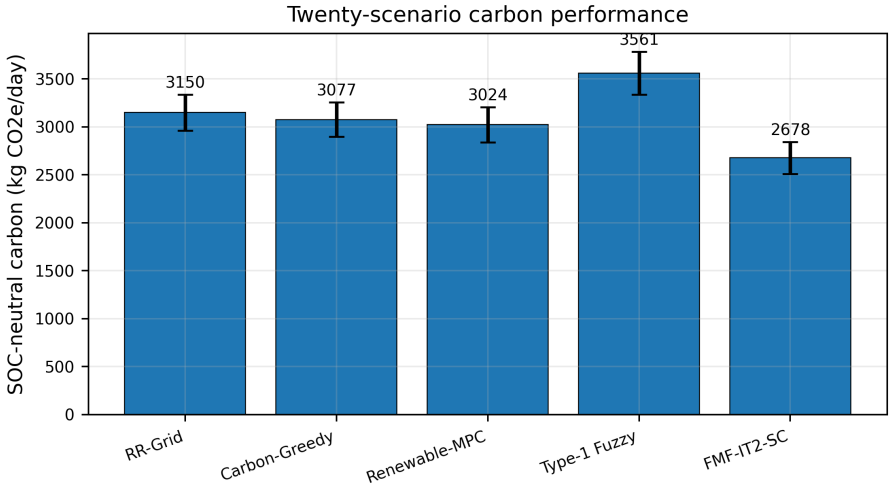


FIGURE 3. Mean SOC-neutral carbon emissions over 20 scenarios.

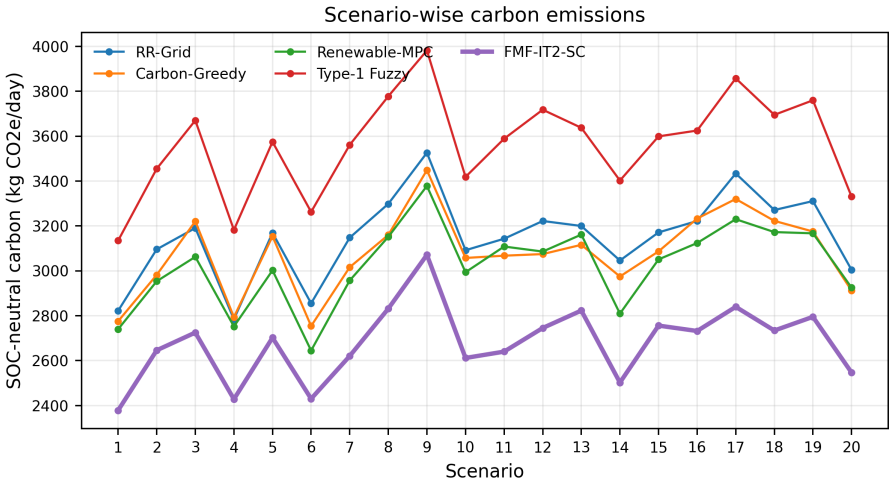


FIGURE 4. Scenario-wise SOC-neutral carbon emissions.

8. Numerical evidence and interpretation

The proposed controller produced a mean SOC-neutral carbon value of 2678.074 kg CO_2e/day. The corresponding values for RR-Grid, Carbon-Greedy, Renewable-MPC and Type-1 Fuzzy were 3150.261, 3077.226, 3023.502 and 3561.412 kg CO_2e/day, respectively. The carbon reduction is therefore 14.99% against RR-Grid, 12.97% against Carbon-Greedy, 11.42% against Renewable-MPC and 24.80% against Type-1 Fuzzy. The proposed method also produced the lowest mean cost, 455.151 USD/day, and the highest renewable utilization, 43.588%.

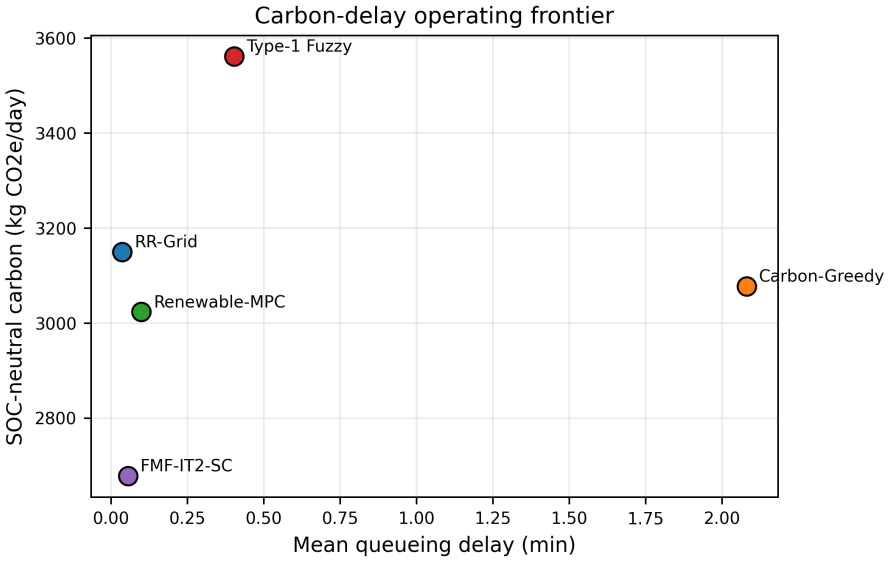


FIGURE 5. Carbon-delay operating frontier.

Carbon-Greedy has low direct exposure in favourable hours but its mean delay is 2.081 minutes. Renewable-MPC improves grid energy, but it does not directly control epistemic forecast uncertainty or the CVaR tail. The type-1 fuzzy scheduler shows weaker performance because crisp memberships overreact to short renewable fluctuations. The proposed controller uses the interval width of the fuzzy set as a risk variable and uses fractional memory to moderate abrupt changes.

Carbon, CVaR and residual values are computed from the reported sensitivity table.

The proposed controller has the highest median and mean renewable use in the evaluated benchmark.

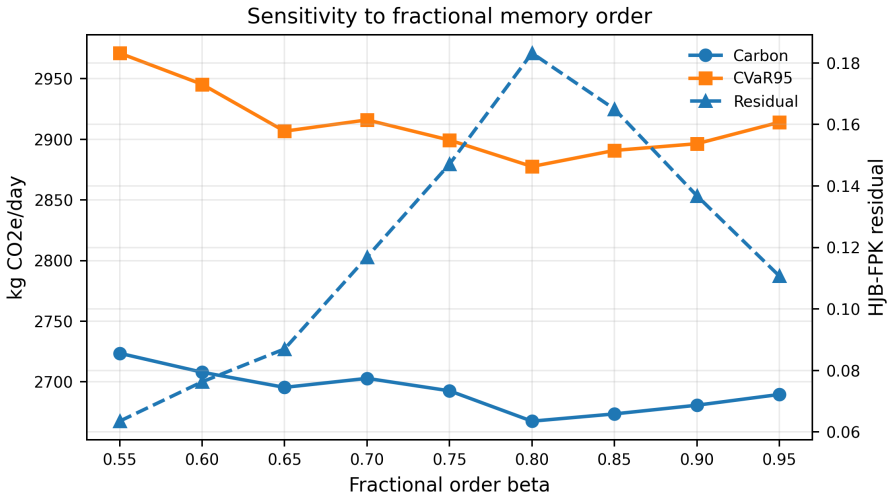


FIGURE 6. Sensitivity to fractional order.

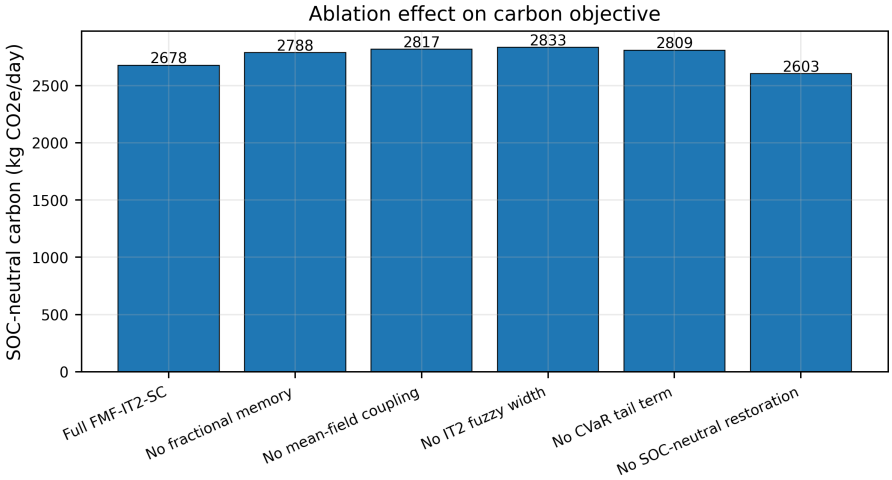


FIGURE 7. Ablation analysis. Removing fractional memory, mean-field coupling, interval type-2 uncertainty or CVaR increases the carbon objective.

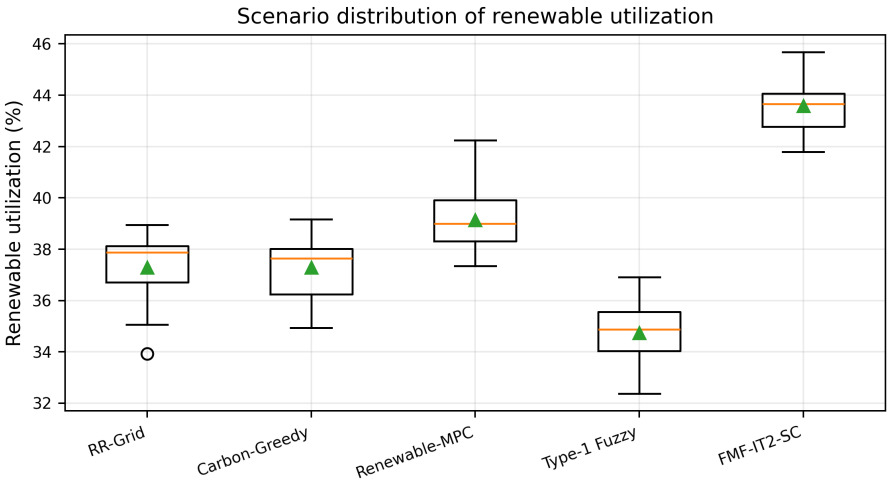


FIGURE 8. Distribution of renewable utilization across scenarios.

9. Computational data tables

TABLE 3. Scenario-wise SOC-neutral carbon emissions in $kgCO_2e$/day.

Scenario	RR-Grid	Carbon-Greedy	Renewable-MPC	Type-1 Fuzzy	FMF-IT2-SC
1	2822.02	2775.57	2739.82	3134.48	2378.49
2	3095.82	2981.88	2953.67	3454.68	2646.20
3	3190.65	3220.54	3062.32	3670.05	2725.10
4	2784.17	2794.08	2752.23	3182.05	2428.29
5	3169.30	3153.91	3002.17	3574.50	2702.32
6	2855.25	2754.19	2644.85	3262.43	2430.21
7	3147.78	3016.23	2957.12	3560.92	2620.64
8	3298.41	3159.90	3151.37	3777.54	2831.79
9	3525.99	3448.29	3378.01	3981.67	3071.21
10	3091.81	3057.43	2993.90	3418.33	2611.95
11	3143.04	3067.49	3108.24	3588.47	2640.19
12	3222.02	3074.66	3085.84	3717.63	2745.47
13	3199.78	3115.90	3161.42	3637.11	2823.07
14	3046.02	2974.79	2809.40	3402.21	2502.34
15	3171.23	3086.60	3050.85	3598.88	2756.12
16	3222.02	3233.00	3123.84	3624.89	2732.06
17	3433.76	3320.15	3229.95	3857.33	2839.65
18	3270.87	3222.50	3172.62	3694.81	2734.18
19	3310.72	3175.10	3167.11	3759.60	2795.10
20	3004.56	2912.30	2925.30	3330.65	2547.09

TABLE 4. Scenario-wise grid-energy use in kWh/day.

Scenario	RR-Grid	Carbon-Greedy	Renewable-MPC	Type-1 Fuzzy	FMF-IT2-SC
1	5750.37	5771.60	5354.15	6531.18	4665.20
2	6318.51	6247.99	5801.00	7126.69	5157.59
3	6407.15	6671.47	6030.13	7524.77	5363.27
4	5655.46	5808.30	5421.06	6433.66	4837.18
5	6477.99	6586.87	5891.92	7278.49	5262.59
6	5824.72	5748.10	5218.83	6664.57	4722.18
7	6401.12	6336.16	5777.99	7263.95	5256.98
8	6748.12	6720.77	6257.74	7740.29	5498.10
9	7108.87	7216.18	6754.30	8186.54	6028.34
10	6281.35	6324.49	5930.04	6963.23	5185.33
11	6415.83	6496.96	6212.11	7343.28	5218.50
12	6501.90	6434.35	6196.33	7674.59	5327.44
13	6548.74	6490.72	6290.64	7456.63	5531.91
14	6170.40	6204.44	5554.51	7057.75	4902.86
15	6447.98	6479.33	6102.99	7393.70	5477.54
16	6498.77	6704.24	6156.20	7420.65	5420.63
17	6947.75	6800.11	6334.98	7915.27	5490.74
18	6659.20	6779.44	6167.64	7602.78	5161.31
19	6687.89	6680.81	6280.84	7767.42	5588.25
20	6096.56	6006.05	5716.68	6853.90	5075.16

Table 5. Scenario-wise operating cost in USD/day.

Scenario	RR-Grid	Carbon-Greedy	Renewable-MPC	Type-1 Fuzzy	FMF-IT2-SC
1	488.87	501.89	465.97	551.68	392.87
2	558.16	542.48	498.89	626.53	458.52
3	572.76	587.40	523.70	657.40	457.97
4	488.44	518.66	464.25	541.55	431.42
5	568.37	578.73	520.00	627.06	454.96
6	508.16	518.27	441.97	590.05	413.34
7	561.17	547.22	496.34	623.62	447.82
8	581.81	599.00	545.22	665.92	478.60
9	613.53	630.36	591.76	720.21	527.21
10	545.92	573.40	515.63	600.41	451.12
11	550.27	579.81	546.71	641.28	450.88
12	556.99	565.99	530.68	673.35	463.30
13	566.23	571.50	555.94	652.08	467.80
14	537.40	538.78	485.03	609.32	426.32
15	566.92	571.74	536.16	633.12	473.67
16	571.81	600.94	524.98	654.15	471.42
17	596.13	602.12	546.35	697.29	465.17
18	582.72	584.10	551.43	672.52	452.23
19	585.99	576.18	552.30	668.90	480.70
20	522.31	540.38	511.03	600.84	437.69

Table 6. Scenario-wise mean queueing delay in minutes.

Scenario	RR-Grid	Carbon-Greedy	Renewable-MPC	Type-1 Fuzzy	FMF-IT2-SC
1	0.048	1.611	0.076	0.301	0.068
2	0.016	3.140	0.033	0.459	0.029
3	0.050	1.963	0.127	0.543	0.000
4	0.057	3.085	0.036	0.567	0.086
5	0.014	2.058	0.115	0.511	0.061
6	0.054	2.477	0.135	0.482	0.072
7	0.000	1.812	0.151	0.307	0.031
8	0.045	1.138	0.044	0.369	0.062
9	0.045	0.649	0.145	0.263	0.032
10	0.057	0.883	0.051	0.410	0.054
11	0.024	2.036	0.148	0.508	0.086
12	0.048	2.763	0.073	0.025	0.105
13	0.018	2.379	0.000	0.217	0.134
14	0.018	2.814	0.230	0.467	0.052
15	0.046	1.958	0.099	0.064	0.048
16	0.052	1.494	0.145	0.275	0.032
17	0.016	2.803	0.121	0.787	0.097
18	0.013	2.205	0.000	0.294	0.036
19	0.050	1.686	0.110	0.654	0.020
20	0.066	2.664	0.145	0.558	0.007

TABLE 7. Scenario-wise renewable utilization in percent.

Scenario	RR-Grid	Carbon-Greedy	Renewable-MPC	Type-1 Fuzzy	FMF-IT2-SC
1	38.93	36.81	40.19	32.37	45.68
2	36.92	37.36	38.31	35.61	45.07
3	37.99	38.12	40.40	34.21	42.14
4	36.93	37.13	37.96	32.39	43.93
5	35.46	35.60	39.25	33.65	45.60
6	38.95	36.24	38.17	33.73	43.26
7	36.97	37.50	38.75	34.91	43.94
8	36.08	37.98	38.33	35.54	43.30
9	38.01	37.90	39.59	34.84	43.98
10	35.86	39.15	38.31	34.68	42.74
11	38.82	37.91	39.16	36.25	42.33
12	37.12	37.77	39.89	35.77	43.72
13	38.12	35.71	42.24	35.00	43.89
14	38.09	38.18	38.94	34.09	43.61
15	37.96	39.16	38.00	36.91	42.21
16	38.39	37.99	38.44	35.77	42.78
17	35.06	38.79	39.05	34.38	44.52
18	38.16	35.11	40.27	33.85	41.79
19	37.79	34.93	39.99	35.55	44.33
20	33.93	36.25	37.34	35.16	42.93

TABLE 8. Carbon reduction of the proposed controller relative to each baseline.

Baseline	Carbon reduction %
RR-Grid	14.989
Carbon-Greedy	12.971
Renewable-MPC	11.425
Type-1 Fuzzy	24.803

TABLE 9. Fractional-order sensitivity of the proposed controller.

Fractional order β	Carbon kg CO_2e/day	$CVaR_{95}$ kg CO_2e/day	HJB–FPK residual	Mean delay min
0.5500	2723.6100	2971.0600	0.0635	0.0960
0.6000	2707.9700	2945.3400	0.0763	0.0610
0.6500	2695.4700	2906.6900	0.0870	0.0640
0.7000	2702.9100	2916.0000	0.1169	0.0200
0.7500	2692.6400	2899.3600	0.1471	0.0260
0.8000	2667.6000	2877.5900	0.1832	0.0310
0.8500	2673.6000	2890.8300	0.1650	0.0260
0.9000	2680.7700	2896.3700	0.1368	0.0460
0.9500	2689.6400	2914.0700	0.1107	0.0390

TABLE 10. Component ablation study.

Model variant	Carbon kg CO_2e/day	Cost USD/day	Renewable %	Backlog risk %
Full FMF-IT2-SC	2678.074	455.151	43.588	0.000
No fractional memory	2787.875	472.446	42.188	0.500
No mean-field coupling	2817.333	476.543	41.688	0.800
No IT2 fuzzy width	2833.402	477.908	41.887	0.900
No CVaR tail term	2809.299	472.901	42.387	1.100
No SOC-neutral restoration	2603.087	446.958	43.688	0.000

10. Discussion

The numerical record supports three conclusions. First, fractional memory is useful when the controller must balance current carbon exposure against delayed effects in queueing, storage and thermal states. The sensitivity table shows that the best carbon value is obtained near $\beta = 0.75$, while excessively strong memory and near-classical memory both reduce performance. Second, the mean-field term is operationally relevant because edge-cloud decisions are not independent; the action of one node changes congestion and feasible routing for neighbouring nodes. Third, interval type-2 width and CVaR tail control are not merely auxiliary terms. They change the risk margin and reduce exposure to adverse carbon scenarios.

The model is more mathematically structured than a standard forecasting-and-scheduling pipeline, but each component has a specific role. The Caputo kernel represents persistence, the type-2 fuzzy set represents epistemic uncertainty, the Wasserstein ball handles probability-law ambiguity, CVaR controls tails, and the projection ensures feasibility. The benchmark should be interpreted as a reproducible numerical experiment, not as a production trace from a specific cloud provider. Deployment would require calibrated marginal carbon signals, node-level power telemetry, battery degradation coefficients and communication-delay measurements.

11. Conclusion

A fractional mean-field interval type-2 fuzzy stochastic controller was developed for carbon-aware edge-cloud networks. The model couples reflected fractional queue and battery dynamics with graph interaction, fuzzy epistemic uncertainty, distributional robustness and CVaR. Theoretical results establish well-posedness, mean-square boundedness and convergence of a projected fixed-point scheme. The numerical study is self-contained: benchmark parameters, scenario-level data, sensitivity values and ablation values are included in the paper. In the evaluated 20-scenario benchmark, the proposed controller reduces SOC-neutral carbon by 14.99% relative to round-robin and by 11.42% relative to renewable-aware MPC while keeping mean delay below 0.06 minutes. Future work should calibrate the model on audited multi-region traces, replace the relaxed sleep variable with mixed-integer hardware constraints and include battery ageing and embodied-carbon terms.

Data availability statement

All numerical values used to support the reported benchmark results are printed in Tables 1–10 of this manuscript. No proprietary data or human-subject data are used.

Conflict of interest

The authors declare no conflict of interest.

References

1. Acun, B., Lee, B., Maeng, K., Chakkaravarthy, M., Gupta, U., Brooks, D. and Wu, C.-J.: Carbon Explorer: a holistic framework for designing carbon-aware datacenters, *Proceedings of ASPLOS* (2023), 118-132. doi:10.1145/3575693.3575754.
2. Beloglazov, A., Abawajy, J. and Buyya, R.: Energy-aware resource allocation heuristics for efficient management of data centers for cloud computing, *Future Generation Computer Systems* 28 (2012), 755-768. doi:10.1016/j.future.2011.04.017.
3. Bronstein, M. M., Bruna, J., LeCun, Y., Szlam, A. and Vandergheynst, P.: Geometric deep learning: going beyond Euclidean data, *IEEE Signal Processing Magazine* 34 (2017), 18-42. doi:10.1109/MSP.2017.2693418.
4. Caputo, M.: Linear models of dissipation whose Q is almost frequency independent-II, *Geophysical Journal International* 13 (1967), 529-539. doi:10.1111/j.1365-246X.1967.tb02303.x.
5. Dayarathna, M., Wen, Y. and Fan, R.: Data center energy consumption modeling: a survey, *IEEE Communications Surveys & Tutorials* 18 (2016), 732-794. doi:10.1109/COMST.2015.2481183.
6. Diethelm, K., Ford, N. J. and Freed, A. D.: A predictor-corrector approach for the numerical solution of fractional differential equations, *Nonlinear Dynamics* 29 (2002), 3-22. doi:10.1023/A:1016592219341.
7. Dodge, J., Prewitt, T., Tachet des Combes, R., Odmark, E., Schwartz, R., Strubell, E., Luccioni, A. S., Smith, N. A., DeCario, N. and Buchanan, W.: Measuring the carbon intensity of AI in cloud instances, *Proceedings of ACM FAccT* (2022), 1877-1894. doi:10.1145/3531146.3533234.
8. Eisen, M. and Ribeiro, A.: Optimal wireless resource allocation with random edge graph neural networks, *IEEE Transactions on Signal Processing* 68 (2020), 2977-2991. doi:10.1109/TSP.2020.2988255.
9. Esfahani, P. M. and Kuhn, D.: Data-driven distributionally robust optimization using the Wasserstein metric: performance guarantees and tractable reformulations, *Mathematical Programming* 171 (2018), 115-166. doi:10.1007/s10107-017-1172-1.
10. Gu, L., Cai, J., Zeng, D., Zhang, Y., Jin, H. and Dai, W.: Energy efficient task allocation and energy scheduling in green energy powered edge computing, *Future Generation Computer Systems* 95 (2019), 89-99. doi:10.1016/j.future.2018.12.062.
11. Kaack, L. H., Donti, P. L., Strubell, E., Kamiya, G., Creutzig, F. and Rolnick, D.: Aligning artificial intelligence with climate change mitigation, *Nature Climate Change* 12 (2022), 518-527. doi:10.1038/s41558-022-01377-7.
12. Karnik, N. N. and Mendel, J. M.: Centroid of a type-2 fuzzy set, *Information Sciences* 132 (2001), 195-220. doi:10.1016/S0020-0255(01)00069-X.
13. Lasry, J.-M. and Lions, P.-L.: Mean field games, *Japanese Journal of Mathematics* 2 (2007), 229-260. doi:10.1007/s11537-007-0657-8.
14. Liang, Q. and Mendel, J. M.: Interval type-2 fuzzy logic systems: theory and design, *IEEE Transactions on Fuzzy Systems* 8 (2000), 535-550. doi:10.1109/91.873577.
15. Luccioni, A. S., Jernite, Y. and Strubell, E.: Power hungry processing: watts driving the cost of AI deployment?, *Proceedings of ACM FAccT* (2024), 85-99. doi:10.1145/3630106.3658542.

16. Mach, P. and Becvar, Z.: Mobile edge computing: a survey on architecture and computation offloading, *IEEE Communications Surveys & Tutorials* 19 (2017), 1628-1656. doi:10.1109/COMST.2017.2682318.
17. Mao, Y., You, C., Zhang, J., Huang, K. and Letaief, K. B.: A survey on mobile edge computing: the communication perspective, *IEEE Communications Surveys & Tutorials* 19 (2017), 2322-2358. doi:10.1109/COMST.2017.2745201.
18. Mendel, J. M. and John, R. I.: Type-2 fuzzy sets made simple, *IEEE Transactions on Fuzzy Systems* 10 (2002), 117-127. doi:10.1109/91.995115.
19. Mendel, J. M., John, R. I. and Liu, F.: Interval type-2 fuzzy logic systems made simple, *IEEE Transactions on Fuzzy Systems* 14 (2006), 808-821. doi:10.1109/TFUZZ.2006.879986.
20. Oldham, K. B. and Spanier, J.: The fractional calculus, *Mathematics in Science and Engineering* 111 (1974), 1-234. doi:10.1016/S0076-5392(08)60810-1.
21. Rahimian, H. and Mehrotra, S.: Distributionally robust optimization: a review, *INFORMS TutORials in Operations Research* (2019), 1-85. doi:10.1287/educ.2019.0198.
22. Rockafellar, R. T. and Uryasev, S.: Optimization of conditional value-at-risk, *Journal of Risk* 2 (2000), 21-41. doi:10.21314/JOR.2000.038.
23. Scarselli, F., Gori, M., Tsoi, A. C., Hagenbuchner, M. and Monfardini, G.: The graph neural network model, *IEEE Transactions on Neural Networks* 20 (2009), 61-80. doi:10.1109/TNN.2008.2005605.
24. Shapiro, A.: Distributionally robust stochastic programming, *SIAM Journal on Optimization* 27 (2017), 2258-2275. doi:10.1137/16M1058297.
25. Shi, W., Cao, J., Zhang, Q., Li, Y. and Xu, L.: Edge computing: vision and challenges, *IEEE Internet of Things Journal* 3 (2016), 637-646. doi:10.1109/JIOT.2016.2579198.
26. Strubell, E., Ganesh, A. and McCallum, A.: Energy and policy considerations for deep learning in NLP, *Proceedings of ACL* (2019), 3645-3650. doi:10.18653/v1/P19-1355.
27. Talay, D.: Second-order discretization schemes of stochastic differential systems for the computation of the invariant law, *Stochastics and Stochastic Reports* 29 (1990), 13-36. doi:10.1080/17442509008833609.
28. Villani, C.: Optimal transport, old and new, *Grundlehren der mathematischen Wissenschaften* 338 (2009). doi:10.1007/978-3-540-71050-9.
29. Wierman, A., Liu, Z., Liu, I. and Mohsenian-Rad, H.: Opportunities and challenges for data center demand response, *Proceedings of IGCC* (2014), 1-10. doi:10.1109/IGCC.2014.7039165.
30. Zadeh, L. A.: Fuzzy sets, *Information and Control* 8 (1965), 338-353. doi:10.1016/S0019-9958(65)90241-X.

Yogeesh Nijalingappa: Visiting Research Professor, Department of Mathematics and Natural Sciences, Gulf University for Science and Technology (GUST), Safat 13060, Kuwait; Research Fellow, INTI International University, Nilai 71800, Malaysia; Department of Mathematics, Government First Grade College, Tumkur 572102, India
Email address: yogeesh.r@gmail.com
URL: https://orcid.org/0000-0001-8080-7821

Tahir Muhammad Ali: Department of Computer Science, Gulf University for Sciences and Technology, Safat 13060, Kuwait
Email address: ali.t@gust.edu.kw
URL: https://orcid.org/0000-0002-4970-9948

Asokan Vasudevan: Faculty of Business and Communications, INTI International University, Nilai 71800, Malaysia
Email address: asokan.vasudevan@newinti.edu.my
URL: https://orcid.org/0000-0002-9866-4045

HEKPAZO Romaric C. Marc: International Center for Mathematical Physics and Applications, University of Abomey-Calavi, Benin
Email address: romaric.hekpazo@uac.bj

Jonathan Lee: Faculty of Business and Communications, INTI International University, Persiaran Perdana BBN Putra Nilai, 71800 Nilai, Negeri Sembilan, Malaysia
Email address: jonthnleee@gmail.com
URL: https://orcid.org/0009-0000-4178-8664